Advances in Materials Technology for Fossil Power Plants
Proceedings from the Seventh International Conference
October 22–25, 2013, Waikoloa, Hawaii, USA
https://doi.org/10.31399/asm.cp.am-epri-2013p1432

D. Gandy, J. Shingledecker, editors

IN-SITU FULL FIELD CREEP DEFORMATION STUDY OF CREEP RESISTANT MATERIALS WELDS

Xinghua Yu, Zhili Feng, Yukinori Yamamoto
Oak Ridge National Laboratory, Oak Ridge, TN, USA

ABSTRACT

The current study proposed a new method that utilizes digital image correlation (DIC) techniques to measure in-situ full field strain maps of creep resistant material welds. The stress-rupture test is performed in a Gleeble™ thermal mechanical simulator. This technique successfully captured a significant difference in the local creep deformation between two Grade 91 steel welds with different pre-welding conditions (standard and non-standard). Strain contour plots exhibited inhomogeneous deformation in the weldments, especially at the heat-affected zone (HAZ). Standard heat-treated specimens had significant creep deformation in the HAZ. On the other hand, non-standard heat treated specimens showed HAZ local strains to be 4.5 times less than that of the standard condition, after a 90-hour creep test at 650°C and 70 MPa. The present study measured the full field strain evolution in the weldments during creep deformation for the first time. The proposed method demonstrated a potential advantage to evaluate local creep deformation in the weldments of any creep resistant material within relatively short periods of time.

INTRODUCTION

Due to the heavy use of fossil fuels, the worldwide annual emission of greenhouse gas from fossil fuel combustion is over 5.4 billion tons [1]. A reduction of CO_2 emission can be achieved by improving power plant efficiency through an increase in steam temperature and pressure. The pressure and temperature combination are referred to as steam parameters. For example, an increase in steam parameters from typical 538°C and 24.1 MPa to 650°C and 34.3 MPa can reduce the energy required by 6.5%, resulting in a commensurate decrease in coal use, and hence a reduction of CO_2 emission [2]. Due to its excellent high temperature creep resistance, creep strength-enhanced ferritic (CSEF) steels (9-12% Cr) are widely used from 600°C to 650°C as tubing and piping in fossil fired power plants to accomplish increased efficiency. In addition, for the last decade, researchers around the world are trying to develop Ultra Advanced Supercritical (U-ASC) materials (stainless steels, Nickel based superalloy), which are aimed at increasing the efficiency of coal-fired power plants by increasing the operating temperature and pressure to 760°C and 35 MPa [3].

The performance of fossil power plant materials however, does not always meet expectations. Nickel based superalloy welds can suffer a significant creep strength reduction [4, 5]. The reduction of creep strength is related to the formation of a precipitate free zone in the weld [6, 7]. ,For CSFF steels There have been reports of numerous failures in the HAZ of after only a few years in service [8, 9, 10, 11]. These failure locations are often traced back to the fine-grained heat affected zone (FGHAZ) of a weld, which experiences a weld thermal cycle with a

peak temperature just above the A_{c3} temperature. It is a well-established fact that non-equilibrium microstructures and their gradients in FGHAZ regions will significantly reduce creep strength [12, 13, 14, 15]. Moreover, the grain size and orientation of the FGHAZ can lead to high tri-axial stress states that may contribute to accelerated creep damage [16,17]. This combination of circumstances leading to premature failure of welded components is discussed in the literature as "Type-IV failures in CSEF steels." Published literature also shows that the creep strength reduction of such joints can be on the order of 40% compared to the base metal [18] for the same service life. The implications of such failures include disruptions of electrical supply, increased cost of electricity, and the potential for failure, endangering the safety of power plant personnel.

Previous research by the current authors showed by applying non-standard tempering (low temperature tempering, LTT) on Grade 91 steel before welding, Type IV failure could be mitigated [19]. The constant creep rate of the non-standard tempering sample were 2.5 times lower than that of standard tempering sample when tested at 70MPa and 650°C. A detailed synchrotron X-ray diffraction study of the HAZ simulated heat-treated samples revealed that the improvement in creep strength was related to the microstructure evolution at FGHAZ [19]. There are many methods proposed to mitigate Type IV failures [30-38], however, the mechanism of Type IV failure is still not clear. One of the difficulties in understanding Type IV failure is that local strain rates can only be estimated by HAZ simulation and followed creep testing [29]. The real strain distribution, which plays an important role in a cross-weld specimen, can hardly be measured during stress-rupture testing.

Digital image correlation (DIC) has been developed and used to measure full field displacement of an object for the last three decades [20]. DIC has been used to measure residual stress [21, 22, 23, 24] , study fatigue [25] and high temperature tensile behavior[26, 27]. This paper presents a novel approach to measuring local deformation in the weldments during creep testing and addresses some of the shortcoming encountered in DIC methods. A Gleeble™ thermal mechanical simulator was used to control stress and temperature during creep testing. A 3D camera system was used to capture the optical images of the sample surface that was coated with a high contrast radom dot pattern. Later the patterns on the sample surface were correlated to one another and strain was calculated as a function of time.

EXPERIMENTAL

Steels and Welding

The chemical composition of ASTM Grade 91 (heat number 30176) is shown in Table 1. After initial thermo-mechanical processing, the steels were normalized at a temperature of 1050°C for 1 h, and then air cooled to room temperature. Two tempering temperatures were investigated in the current study: 760°C (standard) and 650°C (non-standard). The samples were tempered in a furnace for 2 hours, followed by air-cooling to room temperature. These two conditions are designated as HTT (higher pre-weld tempering temperature: 760°C) and LTT (lower pre-weld tempering temperature: 650°C) throughout the text. These two base materials were used for welding and simulated weld thermal cycling experiments.

Two 25.4 mm plates, in the HTT and LTT conditions, were machined on the edge with an angle of 37.5° to make a double-V groove. The grooved plates were pre-heated in a furnace that was set 120°C. Gas tungsten arc welding (GTAW) with argon shielding gas was performed on the plates with one root pass and six fill passes. Inter-pass temperature was kept under 350°C.

Welding current, voltage and speed were 260A, 8V and 2.5mm/s respectively. A 9Cr-1Mo filler wire with 1.6mm in diameter was used. The welded plates were post-weld heat treated (PWHT) in a furnace at 760°C for 2 hours, followed by air-cooling to room temperature. The treated plates were sectioned and machined for creep tests.

Table 1: Chemical composition of the base and weld filler metal (Grade 91).

(wt%)	Fe	C	Mn	Si	Cr	Mo	Ni	V	Nb	N	B
Base	Bal.	0.08	0.27	0.11	8.61	0.89	0.09	0.21	0.07	0.06	<0.001
Filler	Bal.	0.08	0.41	0.31	8.62	0.92	0.15	0.24	0.08	0.04	<0.001

Stress-Rupture Test and Digital Imaging System

Tensile creep-rupture tests of the weld cross-sections were performed using a Gleeble™ thermal mechanical simulator. The system setup is shown in Fig. 1. Samples were machined to 7mm diameter rod with a gage length of 70 mm. The sample was heated to 650°C at 5°C/s and then a constant stress of 70MPa was applied. The total test time was 90 hours. Meanwhile, an in-situ optical image correlation method was used to measure displacement on the surface of an object by tracking random patterns on the samples. Random patterns were created by painting white background and black speckles on the sample surface. Digital cameras (Point Grey GRAS-50S5C-C) linked with a computer were used for image acquisition. Sigma lenses (28-300mm f/3.5-6.3 DG) were used for zooming purpose. External green LED light was used to illuminate the sample surface for better image contrast. Images were taken at 1 minute intervals for the first 12 hours and then at 5 minutes intervals for the subsequent 78 hours. Images were post-processed by the Vic-3D software developed by Correlated Solutions [28] and the strain maps were obtained. The system setup is shown in Fig. 1. The region of interest (ROI), which is about 4mm by 20 mm in area, was selected for strain analysis (Fig.2).

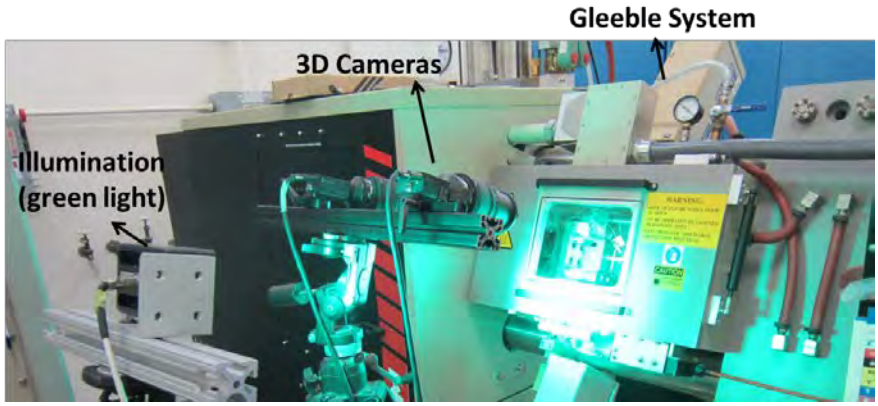

Figure 1. System setup for full field strain measurement during creep deformation

RESULT AND DISCUSSION

Strain Maps Comparison

3D full field strain maps of the ROI and the corresponding sample images are shown in Fig. 2. e_{xx} is the strain along the direction of the load (the horizontal axis). In order to identify different

regions, optical macrographs on the polished and etched surface after testing show the highly deformed regions are in the HAZ. HTT strain maps clearly shows two distinct regions with high strain values after 90 hours of creep. On the other hand, no significant strain localization is observed in the LTT sample. The corresponding optical macrograph indicates the creep deformation is localized in the HAZ (Fig. 2). Detailed microstructural examination in this region s required in future work to obtain a full understanding of the mechanism affecting the microstructure.

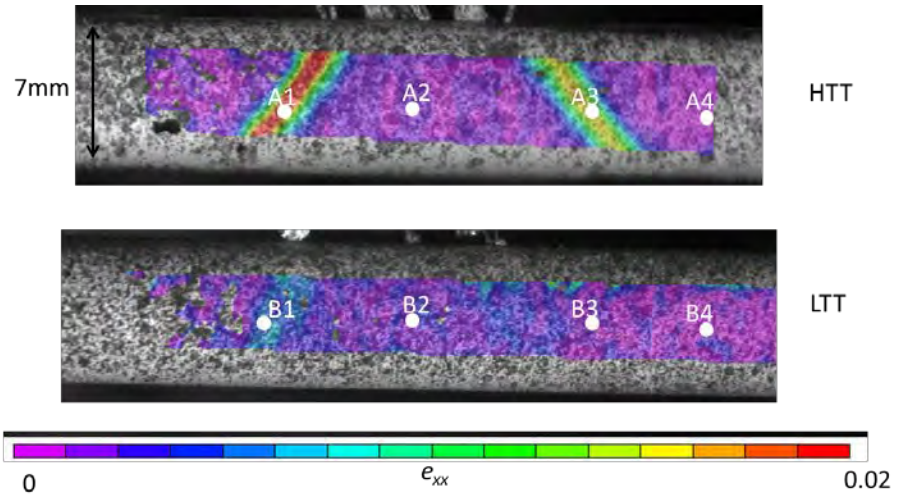

Figure 2. Full field strain maps (e_{xx}) obtained using DIC showing deformation of HTT and LTT cross-weld sample after 90 hours creep deformation

In order to understand the local strain development as a function of time, four circular ROIs were further selected on each strain map (A1-A4 and B1-B4 as shown in Fig.2). Four circular regions 0.5 mm in diameter depicted in the figure represent the left HAZ, weld metal, right HAZ and base metal. Strain vs. time is shown in Fig. 3. For the HTT sample, there is very little creep deformation observed in the weld metal and the base metal, whereas creep deformation in the left and right HAZ is significant with almost the same strain rate (4.5×10^{-8}/s) in the range of current testing. For the LTT sample, no obvious creep deformation is observed in the base metal, but slight deformation is seen in the weld metal. The reason for the deformation of weld metal in the LTT sample is unknown and needs to be further investigated. Though the strain map of the LTT sample in Fig. 2 does not show the apparent difference in local deformation at the HAZ, high strain rate of HAZ is still observed (1.0×10^{-8}/s). Previous stress-rupture tests have shown that creep life of the HTT sample is approximately 5 times lower than that of LTT sample [19]. Surprisingly, the strain rate HAZ of the HTT sample is approximately 5 times higher than that of LTT, indicating that the local strain rate at the HAZ could be associated with creep life of the cross-weld specimens. Further detailed studies of the local deformation characteristics are currently in progress.

The strain (e_{xx}) traverse plots along the lines A1-A4 and B1-B4 after 90 hours of creep were shown in Fig. 4. Clearly, the two peaks of the HTT strain plot are due to the significant creep in the the HAZ. The width of the peak is approximately 4mm, which is larger than the measured width of the HAZ which is approximately 2mm [29]. As a result, this high strain rate region may include both FGHAZ and ICHAZ. On the other hand, the spike in the LTT strain traverse plot is just above the noise level. The width of the peak in the LTTcurve is also approximately 4mm.

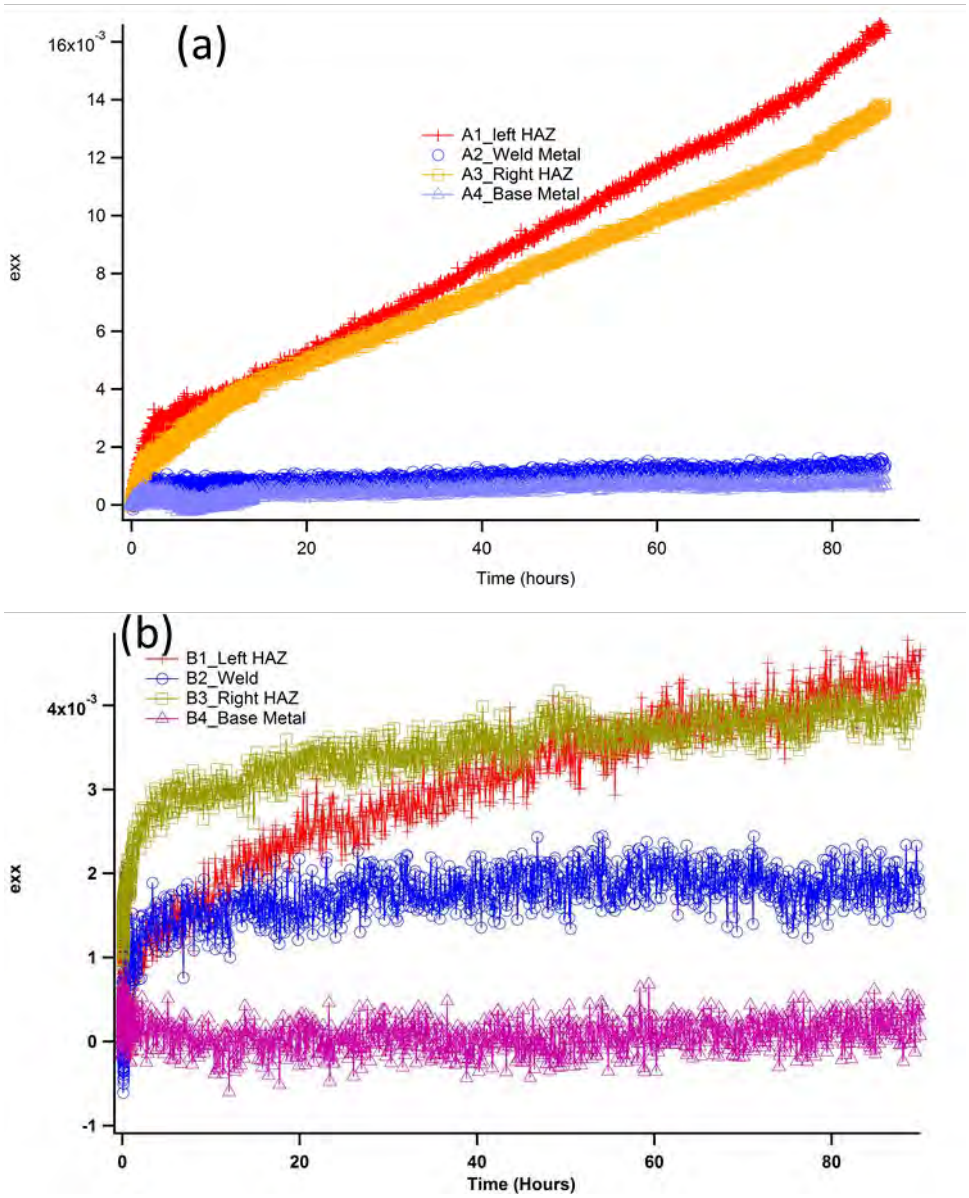

Figure 3. Local strain evolution as a function of time during creep

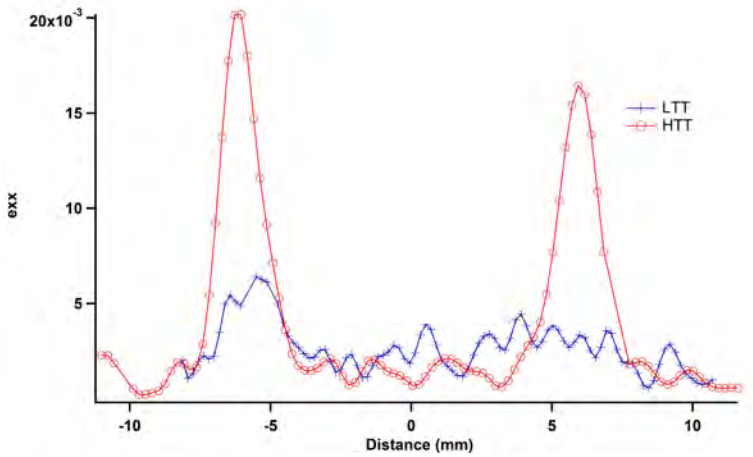

Figure 4. Traverse strain plot comparison between HTT and LTT

Advantages of Current Measurement System

Fig. 5 shows the strain vs. time curves of the LTT and HTT welds of conventional creep tests at 650°C and 70MPa, for up to 90 h [19]. No significant difference is found in the creep curves between the LTT and HTT samples. Final strain at 90 hours is 0.24 for the HTT sample and 0.20 for the LTT sample. However, local strain in the HAZ measured by DIC is much higher than overall strain (Fig. 3). In addition, the LTT sample shows superior creep performance after the 90 hours test.

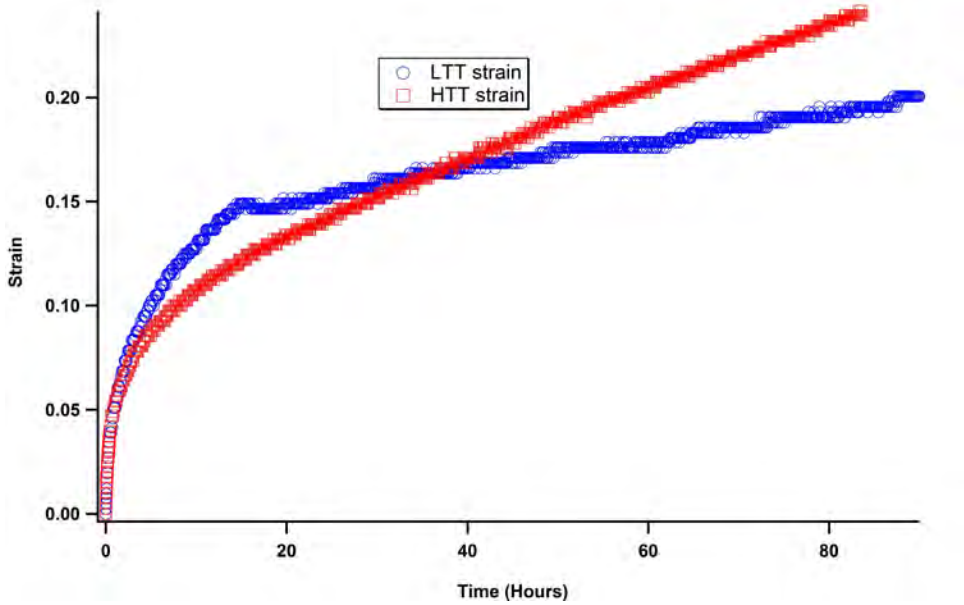

Figure 5. Creep curve comparison between LTT and HTT cross weld samples

In conventional stress-rupture tests, the overall strain of the cross-weld specimen is composed of the deformations from weld metal, HAZ and base metal, due to the microstructure gradient in the weldments. Usually, the creep resistance at the HAZ of CSEF steels, especially the FGHAZ/ICHAZ, is very low, because of its weakened microstructure but the local creep deformation can hardly be separated by using the conventional creep testing. The current study successfully proved that the Gleeble and DIC system can map the full strain field with a resolution of 200μm, and the local strain rate can be correlated to the corresponding microstructure. Another advantage of the 3-D camera method is to obtain the local strain rate distribution within a relatively short test period. For example, it took thousands of hours to see the difference between the LTT and the HTT samples at the same creep test condition used in the current study [19]. However, the current system focused only on the secondary creep regime, so that it could easily differentiate the local strain rates of the HTT and LTT samples after only 90 h of testing. There are many factors that affect the creep performance of the weldments of CSEF: weld metal strength [30]; fusion welding process, joint design [31,32]; solid state welding design [33]; base metal composition [34, 35, 36, 37]; base metal heat treatment [19, 30] etc. Evaluation of the effects of these welding processes or material compositions on creep properties will involve tens of thousands of hours of stress-rupture testing. The current stain mapping system could significantly reduce the total test time.

The present study used Grade 91 steel as an example and shows the advantage of the Gleeble and DIC system to measure full field strain distributions during creep. The same approach can also be used to evaluate other heat resistant alloy welds for creep performance.

CONCLUSIONS

A Gleeble^{TM} thermal mechanical simulator and a DIC system has successfully been used to measure *in-situ* full field strain maps of cross-weld Grade 91 steel samples. The spatial resolution of the strain map is about 200μm. Results show creep deformation is mostly concentrated in the HAZ. Local strain rate for the HAZ, weld metal and base metal was plotted as a function of time. The HTT sample showed significant deformation in the HAZ compared to the LTT sample. The present measuring system, which has the advantage of evaluating creep performance of the weld in a short period of time, can also be used to evaluate weld creep performance of other creep resistant alloys.

ACKNOWLEDGMENTS

The authors acknowledge the materials from U.S. Department of Energy, Office of Fossil Energy, Fossil Energy Advanced Research Materials Program, under contract DE-AC05-00OR22725 with UT-Battelle, LLC. Mr. Tom Muth is thanked for his review and comments on this manuscript.

REFERENCES

[1] Cole, D.G.. “Design of Heat-Resistant Steels for Small Power Plant” Doctoral Dissertation, University of Cambridge, UK, (2000)

[2] Abe, F. “Precipitate design for creep strengthening of 9% Cr tempered martensitic steel for ultra-supercritical power plants” Science and Technology of Advanced Materials, Vol 9. (2008) pp. 013002

[3] R.Viswanathan, R.Purgert, S.Goodstine, J.Tanzosh, G.Stanko, J.P. Shingledecker, B.Vitalis "U.S. Program on Materials Technology for Ultrasupercritical Coal-Fired Boilers" Advances in Materials Technology for Fossil Power Plants: Proceedings of the 5th International Conference 2008 ASM International
[4] M. Santella, J. Shingledecker, B. Swindeman "Materials for Advanced Ultra-Supercritical Steam Boilers" 24th Annual Conference on Fossil Energy Materials Pittsburgh, PA, May 26, 2010.
[5] P.F. Tortorelli, Y. Yamamoto, P.J. Maziasz, J.L. Moser, C.O. Stevens, M.L.Santella J.P. Shingledecker. " Materials for Advanced Ultra-Supercritical (A-USC) Steam Boilers" 26th Annual Conference on Fossil Energy Materials, Pittsburgh, Pennsylvania April 19, 2012
[6] D. Tung, J. C. Lippold, "Weld Solidification Behavior of Inconel Alloy 740H" Welding and Repair Technology for Power Plants, Tenth International EPRI Conference
[7] D. H. Bechetti, "Microstructure Evolution and Creep Rupture Behavior of INCONEL Alloy 740H Fusion Welds" PhD dissertation, Lehigh University, 2013
[8] Shibli, I.A., "Performance of P91 Thick Section Welds Under Steady and Cyclic Loading Conditions: Power Plant and Research Experience", OMMI, Vol. 1, No. 3 (2002), pp. 1-17.
[9] J.F. Henry. Combined Cycle Journal, First Quarter (2005) 8
[10] I.A. Shibli, K. Coleman, www.ommi.co.uk/etd/ETD-EPRI-%20P91%20Failures.pdf
[11] F. J. Berte, Combined Cycle Journal, Second Quarter (2007) 52
[12] J.A. Francis, W. Mazur, H. K. D. H. Bhadeshia, Mater. Sci and Technol. 22 (2006) 1387
[13] F. Abe, M. Tabuchi, Mater Sci and Technol., 9 (2004) 22
[14] H. Hirata, K. Ogawa, Weld. Int, 19 (2005) 37
[15] H. Hirata, K. Ogawa, Weld. Int, 19 (2005) 118
[16] S.K. Albert, M. Matsui, T. Watanabe, H. Hongo, K. Kubo, M. Tabuchi, Int. J. Press. Vessel. Pip., 80 (2003) 405
[17] D. Li, K. Shinozaki, H. Kuroki, Mater. Sci. Technol. 19 (2003) 1253
[18] Y. Otoguro, M. Matsubara, I. Itoh, T. Nakazawa, Nucl. Eng. Des., 196 (2000)51
[19] X. Yu, S. S. Babu, H. Terasaki, Y. Komizo, Y. Yamamoto, M. Santella. "Correlation of Precipitate Stability to Increased Creep Resistance of Cr-Mo Steel Welds" Acta Materialia Volume 61, Issue 6, April 2013, Pages 2194–2206
[20] Y. Yamamoto, S. S. Babu, M. Santella, X. Yu "Improving the Performance of Creep Strengthen-Enhanced Ferritic Steeels" 27th Annual Conference on Fossil Energy Materials Pittsburgh, Pennsylvania, 2013
[21] M. A. Sutton, J. Orteu, H. W. Schreier, "Image Correlation for Shapes, Motion and Deformation Measurement" pringer Science+Business Media, LLC, 233 Spring Street, New York, NY 10013, USA
[21] D. V. Nelson, A. Makino, and T. Schmidt, "Residual stress determination using hole drilling and 3D image correlation," Exp. Mech.46, 31–38 (2006).
[22] M. J. McGinnis, S. Pessiki, and H. Turker, "Application of three-dimensional digital image correlation to the core- drilling method," Exp. Mech. 45, 359–367 (2005).
[23] J. D. Lord, D. Penn, and P. Whitehead, "The application of digital image correlation for measuring residual stress by incremental hole drilling," Appl. Mech. Mater. 13–14, 65–73 (2008).
[24] J. Gao, H. Shang "Deformation-pattern-based digital image correlation method and its application to residual stress measurement." Appl Opt. 2009 Mar 1;48(7):1371-81.
[25]T. Niendorf, J. Dadda, D. Canadinc, H.J. Maier, I. Karaman "Monitoring the fatigue-induced damage evolution in ultrafine-grained interstitial-free steel utilizing digital image correlation" Materials Science and Engineering A 517 (2009) 225– 234

[26]X. Chen, N. Xu, L. Yang, D. Xiang "High temperature displacement and strain measurement using a monochromatic light illuminated stereo digital image correlation system" Meas. Sci. Technol. 23 (2012) 125603
[27]B. Pan1, D.Wu, Z.Wang Y. Xia "High-temperature digital image correlation method for full-field deformation measurement at 1200 C" Meas. Sci. Technol. 22 (2011) 015701
[28] Correlated Solutions, West Columbia, South Carolina. <www.correlatedsolutions.com>.
[29] X. Yu, "Multi-Scale Characterization of Heat-Affected Zone in Martensitic Steels" PhD dissertation, The Ohio State University, 2012
[30] P. Mayr, S. Mitsche, H. Cerjak, S. Allen "The Impact of Weld Metal Creep Strength on the Overall Creep Strength of 9% Cr Steel Weldments" Journal of Engineering Materials and Technology APRIL 2011, Vol. 133 / 021011-1
[31] J. A. Francis, G. M. D. Cantin, W. Mazur and H. K. D. H. Bhadeshia "Effects of weld preheat emperature and heat input on type IV failure" Science and Technology of Welding and Joining 2009 VOL 14 NO 5 436-442
[32] S. K. Albert, M. Tabuchi, H. Hongo, T. Watanabe, K. Kubo M. Matsui "Effect of welding process and groove angle on type IV cracking behaviour of weld joints of a ferritic steel" Science and Technology of Welding and Joining 2005 VOL 10 NO 2 149-157
[33] G grant, J, Darsell, B. Jonsson, F. Rave, D. Chandrasekaran, J. Merta, C. Widner, M. West, B. Jasthi, I. Markon " Joining Technologies for Coal Power Applications" The 26th Annual Conference on Fossil Energy Materials, Pittsburgh, Pennsylvania April 19, 2012
[34] S. K. Albert, M. Kondo, M. Tabuchi, F. Yin, K. Sawada, F. Abe "Improvi ng the Creep Properties of 9Cr-3W-3Co-NbV Steels and their Weld Joints by the Addition of Boron" METALLURGICAL AND MATERIALS TRANSACTIONS A VOLUME 36A, FEBRUARY 2005—333-343
[35] Tsukamoto, S., Liu, Y., Shirane, T., Tabuchi, M., Abe, F., " Improvement of Microstructure Stability during Creep in High Cr Ferritic Heat Resistant Steel HAZ" Trends in Welding Research Proceeding of 9th International Conferenc, Chicago, 2012
[36] K. Sawada, M. Taneike, K. Kimura and F. Abe, "Effect of Nitrogen Content on Microstructural Aspects and Creep Behavior in Extremely Low Carbon 9Cr Heat-resistant Steel", The Iron and Steel Institute of Japan(ISIJ) International, Vol. 44(7), 2004, pp. 1243-1249.
[37] M. Ohgami, H. Minura, and H. Naoi, "Creep Rupture Properties and Microstructures of a New Ferritic W Containing Steel", Proceedings of the Fifth International Conference on Creep of Materials, Lake Buena Vista, Florida, 18-21 May, 1992, pp. 69-73.